0090-9556/08/3608-1562–1569$20.00
DRUG METABOLISM AND DISPOSITION
Vol. 36, No. 8
20560/3363129
Printed in U.S.A.

DMD 36:1562–1569, 2008

UDP-Glucuronosyltransferase 1A6 Is the Major Isozyme Responsible for Protocatechuic Aldehyde Glucuronidation in Human Liver Microsomes

Hui-Xin Liu, Yong Liu, Jiang-Wei Zhang, Wei Li, Hong-Tao Liu, and Ling Yang

Laboratory of Pharmaceutical Resource Discovery (H.-X.L., Y.L., J.-W.Z., W.L., H.-T.L., L.Y.), Dalian Institute of Chemical Physics, Chinese Academy of Sciences, Dalian, China; and Graduate University of Chinese Academy of Sciences, Beijing, China (H.-X.L., J.-W.Z., W.L., H.-T.L.)

Received January 28, 2008; accepted May 9, 2008

ABSTRACT:

Glucuronidation is an important pathway in the metabolism of protocatechuic aldehyde (3,4-dihydroxybenzaldehyde, PAL). However, the metabolites and primary UDP-glucuronosyltransferase (UGT) isozymes responsible for PAL glucuronidation remain to be determined in human. Here, we characterized PAL glucuronidation by human liver microsomes (HLMs), human intestine microsomes (HIMs), and 12 recombinant UGT (rUGT) isozymes to identify what kinds of metabolites are present and which human UGT isozymes are involved. Two metabolites (M-1 and M-2) were detected in reactions catalyzed by HLMs, HIMs, rUGT1A6, and rUGT1A9 and were identified as monoglucuronides by liquid chromatography-mass spectrometry. A kinetic study showed that PAL glucuronidation by rUGT1A6, rUGT1A9, HIMs, and HLMs followed Michaelis-Menten kinetics. The K_m values of HLMs, HIMs, rUGT1A6, and rUGT1A9 for PAL glucuronidation were as follows: 432.7 ± 24.5, 626.9 ± 49.2, 367.5 ± 25.1, and 379.9 ± 42.5 μM for M-1 and 336.7 ± 15.3, 494.3 ± 48.7, 211.4 ± 13.4, and 238.5 ± 26.2 μM for M-2, respectively. The PAL glucuronidation activity was significantly correlated with UGT1A6 activity rather than with UGT1A9 activity from 15 individual HLMs. A chemical inhibition study showed that the IC_{50} for phenylbutazone inhibition of PAL glucuronidation was similar in HLMs (61.9 ± 7.9 μM) compared with rUGT1A6 (45.3 ± 7.7 μM). In contrast, androsterone inhibited rUGT1A9-catalyzed and HLM-catalyzed PAL glucuronidation with IC_{50} values of 27.1 ± 3.8 and >500 μM, respectively. In combination, we identified UGT1A6 as the major isozyme responsible for PAL glucuronidation in HLMs.

Glucuronidation represents a major phase II reaction of numerous xenobiotic as well as endogenous compounds (King et al., 2000). By adding the glucuronosyl group of UDP-glucuronic acid (UDPGA), which is catalyzed by a superfamily of UDP-glucuronosyltransferases (UGTs), such compounds become more hydrophilic and are therefore more readily excreted. Currently, at least 17 human UGTs have been identified and are classified into the two subfamilies, UGT1 and UGT2, based on sequence homologies (Radominska-Pandya et al., 1999; Mackenzie et al., 2005). The majority of UGTs, as with other xenobiotic-metabolizing enzymes, display broad and overlapping substrate specificities. But a few specific reactions have been described for certain UGT isoforms, e.g., the glucuronidation of bilirubin by UGT1A1 (Bosma et al., 1994), trifluoperazine by UGT1A4 (Di Marco et al., 2005), serotonin by UGT1A6 (Krishnaswamy et al., 2003), propofol by UGT1A9 (Ebner et al., 1993), and 3′-azido-3′-deoxythymidine by UGT2B7 (Court et al., 2003). UGTs are not limited to the liver, and some extrahepatic tissues are known to exhibit significant activities. For example, UGT1A7, 1A8, and 1A10 are specifically expressed in the gastrointestinal tract with little or no activity in the liver (Strassburg et al., 1999).

Salvia miltiorrhiza has been widely used in China for the treatment of coronary heart disease, cerebrovascular disease, bone loss, hepatitis, hepatocirrhosis, and chronic renal failure (Sugiyama et al., 2002; Ding et al., 2005; Chang et al., 2006). PAL (Fig. 1) has been considered as one of the major active constituents of *S. miltiorrhiza* (Ye et al., 2003). A number of pharmacological studies showed that PAL possessed biological activities such as reducing inflammation, reducing atherosclerosis, improving the microcirculation, and inhibiting the aggregation of platelets (Han et al., 2005; Zhou et al., 2005). In general, the water-soluble curative components of *S. miltiorrhiza* including PAL are obtained by water extraction from the medicinal herb and then are orally administrated. This class of components was called water-soluble phenolic acids and was likely to go through phase II conjugation reactions (Baba et al., 2004; Konishi et al., 2005). Phase II reactions lead to the formation of a covalent linkage between a functional group either on the parent compound or on one introduced as a result of a phase I reaction (Iyanagi, 2007). The conjugation reactions, sulfation, methylation, and glucuronidation, catalyzed

This work was supported by the National Natural Science Foundation of China (30630075 and 30772608) and by the Dalian Institute of Chemical Physics Innovation Fund of Chinese Academy of Sciences and Ph.D. Exploring Fund (S200628).

Article, publication date, and citation information can be found at http://dmd.aspetjournals.org.

doi:10.1124/dmd.108.020560.

ABBREVIATIONS: UDPGA, uridine-5′-diphosphoglucuronic acid; UGT, UDP-glucuronosyltransferase; PAL, protocatechuic aldehyde; ST, sulfotransferase; COMT, catechol-*O*-methyltransferase; HLM, human liver microsome; HIM, human intestinal microsome; rUGT, recombinant UGT; SAM, *S*-adenosyl-L-methionine; PAPS, 3′-phosphoadenosine 5′-phosphosulfate; HPLC, high-performance liquid chromatography.

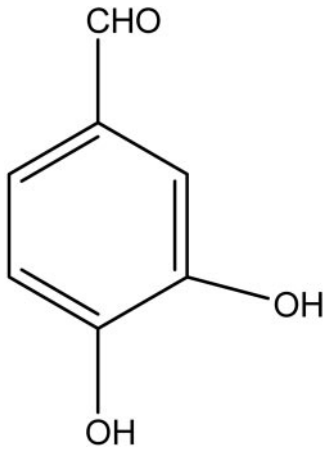

FIG. 1. Structure of PAL.

by sulfotransferases (STs), catechol-*O*-methyltransferases (COMTs), and UGTs, respectively, are effective detoxication mechanisms and allow the excretion of the conjugates into bile and urine (Antonio et al., 2002). Glucuronidation of PAL has been detected in studies with rats (Xu et al., 2007a,b). Studies have shown that the majority of metabolites were present in the plasma as conjugated forms and reached a maximum concentration at 15 min after PAL administration (Xu et al., 2007b). However, detailed information on the metabolism of PAL and their pharmacokinetic fate in human is still scant.

Identification of metabolites and enzymes responsible for drug metabolism are important to understand which one, parent drug or metabolite(s), is really active and how variations in drug concentrations can lead to differences in drug efficacy and toxicity. In addition, the identification of drug-metabolizing enzymes will be helpful for elucidating the role of these particular enzymes in drug-drug interactions and evaluating the impact of genetic polymorphisms associated with the enzymes of interest. Currently, the strategies for the procedures typically used for definitive cytochrome P450 reaction phenotyping have been developed for the identification of human UGTs based on the glucuronidation of endogenous and exogenous compounds in vitro (Bauman et al., 2005; Mano et al., 2007).

In present study, the conjugation pathway of PAL in human was distinguished in vitro. We detected two monoglucuronide metabolites produced by HLMs, HIMs, and two rUGTs (rUGT1A6, and rUGT1A9) by liquid chromatography-mass spectrometry. We identified UGT1A6 as the major isozyme involved in PAL glucuronidation catalyzed by HLMs by the following evidence: 1) 12 rUGT isozymes, 2) correlation analysis, and 3) chemical inhibition study.

Materials and Methods

Chemicals and Reagents. Protocatechuic aldehyde, alamethicin, magnesium chloride, D-saccharic acid 1,4-lactone, β-D-glucuronoside, UDPGA, serotonin, propofol, androsterone, *S*-adenosyl-L-methionine (SAM), 3′-phosphoadenosine 5′-phosphosulfate (PAPS), and phenylbutazone were purchased from Sigma-Aldrich (St. Louis, MO, USA). HLMs and human liver S9 fraction were prepared according to the methods described by Guengerich (1989). Protein concentration was determined by using bovine serum albumin as the standard (Lowry et al., 1951). Pooled HIMs containing equal amounts of microsomes prepared from both the duodenum and jejunum section of each of the five donors (one female and four males of Caucasian and African American race, with ages ranging from 16 to 64 years) and a panel of recombinant human UGT Supersomes (UGT1A1, 1A3, 1A4, 1A6, 1A7, 1A8, 1A9, 1A10, 2B4, 2B7, 2B15, and 2B17) expressed in baculovirus-infected insect cells were purchased from BD Gentest Corp. (Woburn, MA). The range of catalytic rate activity for 12 recombinant UGT Supersomes supplied by the company were from 250 to 12,000 pmol/min/mg of protein. All other reagents were of HPLC grade or of the highest grade commercially available.

Incubations of PAL with Human Liver S9 Fraction. Methylation of PAL was evaluated by incubating PAL (100 μM) with human liver S9 (2 mg of protein/ml), $MgCl_2$ (5 mM), and SAM (50 μM) in a total volume of 200 μl of 50 mM Tris-HCl buffer (pH 7.5) at 37°C for 30 min. The reactions were terminated by the addition of 0.1 ml of 10% trichloroacetic acid, followed by centrifugation at 20,000*g* for 10 min to obtain the supernatant. Aliquots (30 μl) were then analyzed by a high-performance liquid chromatograph equipped with a UV detector. Control incubations without SAM or without substrate were performed to ensure that the metabolites produced were human liver S9 and were SAM-dependent or not. Sulfation of PAL was evaluated by incubating PAL (100 μM) with human liver S9 (2 mg of protein/ml) and PAPS (50 μM) in a total volume of 200 μl of 50 mM Tris-HCl buffer (pH 6.8) at 37°C for 30 min. The reactions were terminated by the addition of 0.1 ml of 10% trichloroacetic acid, followed by centrifugation at 20,000*g* for 10 min to obtain the supernatant. Aliquots (30 μl) were then analyzed by HPLC. Control incubations without PAPS or without substrate were performed to ensure that the metabolites produced were human liver S9 fraction and were PAPS-dependent or not.

Identification of PAL Glucuronidation. PAL (400 μM) was incubated in reaction mixtures of 0.20 ml of 50 mM Tris-HCl buffer (pH 7.5) containing 5 mM $MgCl_2$, 25 μg/ml alamethicin, 10 mM D-saccharic acid 1,4-lactone, and HLMs at 37°C for 20 min in the presence of 5 mM UDPGA. The reactions were terminated by the addition of 0.1 ml of 10% trichloroacetic acid, followed by centrifugation at 20,000*g* for 10 min to obtain the supernatant. Aliquots (30 μl) were then analyzed by HPLC. Control incubations without UDPGA or without substrate or without microsomes were performed to ensure that the metabolites produced were microsomes and were UDPGA-dependent or not. For the identification of the glucuronide peaks in HPLC, enzymatic hydrolysis was performed with some incubations. In these experiments, D-saccharic acid 1,4-lactone was omitted, and an aliquot of the incubation mixture was mixed with an equal volume of 0.15 M acetate buffer (pH 5.0) containing 1800 Fishman units of β-D-glucuronidase and incubated for 2 h at 37°C before HPLC analysis. Liquid chromatography-mass spectrometry was also used for the identification of PAL metabolites. The HPLC eluent from the detector was introduced into the mass spectrometer via a 1:4 split. The mass spectrometer was a TSQ triple quadrupole (Thermo Fisher Scientific, Waltham, MA) equipped with an electrospray ionization interface. The spray voltage was 4.5 kV, and the capillary temperature was 300°C. Nitrogen was used as the nebulizing and auxiliary gas. The nebulizing gas backpressure was set at 40 psi and auxiliary gas at 20 (arbitrary units). Initially, the mass spectrometer was programmed to perform full scans between *m/z* 100 and 1000 to observe the $[M - H]^-$ signals.

Kinetic Study in HLMs and HIMs. PAL (25–2000 μM) was preincubated with pooled HLMs (0.1 mg of protein/ml) and HIMs (0.15 mg of protein/ml) at 37°C for 3 min in a final volume of 0.20 ml of 50 mM Tris-HCl buffer (pH 7.5) containing 5 mM $MgCl_2$, 10 mM D-saccharic acid 1,4-lactone, and 25 μg/ml alamethicin. After preincubation of the reaction mixture, the reaction was started by adding UDPGA to a final concentration of 5 mM. After incubation at 37°C for 20 min, the reaction was terminated by the addition of 0.1 ml of 10% trichloroacetic acid containing 24 μg of internal standard (240 μg/ml *p*-nitrophenyl-β-D-glucuronide), followed by centrifugation at 20,000*g* for 10 min to obtain the supernatant. Aliquots (30 μl) were then analyzed by HPLC. As no PAL monoglucuronide standards were available, it was assumed that the glucuronides of PAL had the same molar absorbance as the respective aglycones.

Glucuronidation by Recombinant UGTs. PAL glucuronidation was measured in reaction mixtures containing recombinant human UGT1A1, 1A3, 1A4, 1A6, 1A7, 1A8, 1A9, 1A10, 2B4, 2B7, 2B15, and 2B17. Substrate concentrations of 400 μM and protein concentrations of 0.1 mg of protein/ml were used. All of the isozymes were left to react for 20 min. A kinetic study for PAL glucuronidation by rUGT1A6 and rUGT1A9 was also conducted by incubating PAL with rUGT1A6 (0.1 mg of protein/ml) or rUGT1A9 (0.1 mg of protein/ml) for 20 min. The ranges of substrate concentration used to obtain kinetic profiles were 25 to 2000 μM in both rUGT1A6 and rUGT1A9.

Correlation Analysis in HLMs. The glucuronidation of PAL was measured in microsomes of 15 individual human livers. The activity of UGT1A6-

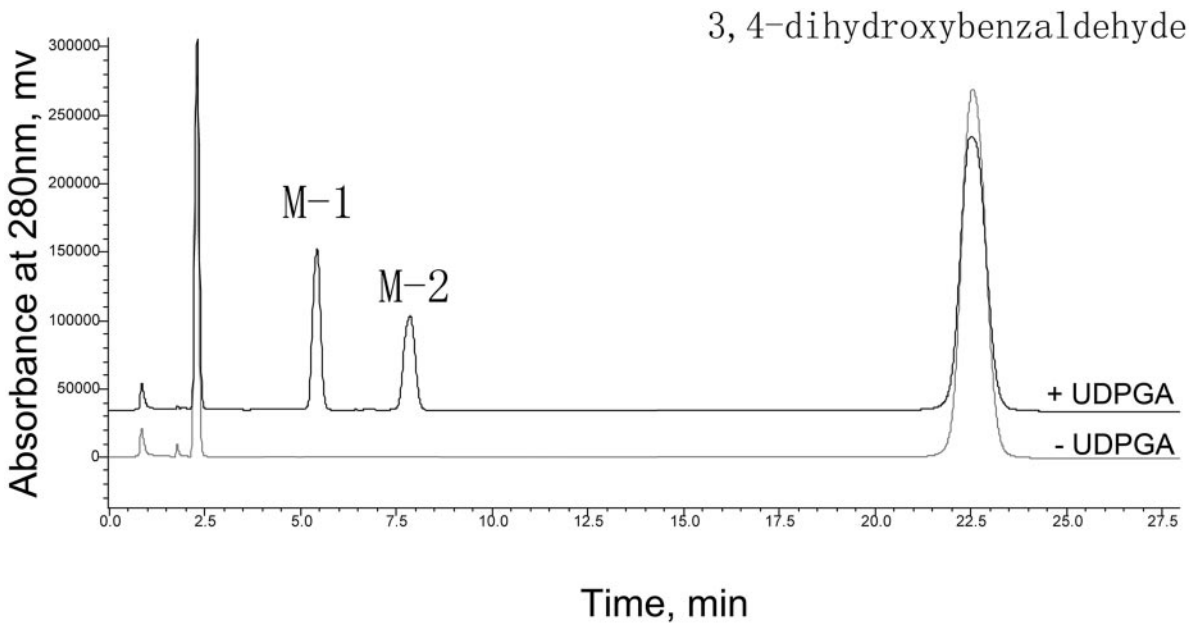

FIG. 2. Representative HPLC profiles of PAL and its metabolites. PAL (500 μM) was incubated with HLMs (0.1 mg/ml) at 37°C for 30 min with (+UDPGA) or without (−UDPGA) UDPGA as described under *Materials and Methods*. Metabolites (M-1 and M-2) and PAL were eluted at 5.4, 7.9, and 22.9 min, respectively.

catalyzed serotonin glucuronidation and UGT1A9-catalyzed propofol glucuronidation was 1.57 to 3.71 and 0.70 to 2.37 nmol/min/mg of protein, respectively. The substrate and HLMs concentrations were 400 μM and 0.1 mg of protein/ml, respectively. The reaction mixture was incubated for 20 min at 37°C. Glucuronidation activities of serotonin and of propofol were provided by the manufacturer as typical reference activities for UGT1A6 and UGT1A9, respectively. $p < 0.05$ was considered statistically significant.

Chemical Inhibition Studies. PAL glucuronidation in pooled HLMs, rUGT1A6, and rUGT1A9 was measured in the absence or presence of either phenylbutazone or androsterone, two potent inhibitors for UGT1A6 and for UGT1A9, respectively (Uchaipichat et al., 2006). PAL (400 μM) was incubated in the absence or presence of either phenylbutazone (0–750 μM) or androsterone (0–500 μM). Incubation was performed for 20 min using a protein concentration of 0.1 mg of protein/ml.

Assay. The peak areas of PAL glucuronidation and the internal standard were analyzed by HPLC with a UV detector. The HPLC system (Shimadzu, Kyoto, Japan) consisted of a SCL-10A system controller, two LC-10AT pumps, a SIL-10A auto injector, and a SPD-10AVP UV detector and a RP Luna (Phenomenex, Torrance, CA) C_{18} column (4.6 × 150 mm, 5 μm) was used to separate PAL and its metabolites. An isocratic mobile phase system was used. Eluent A was acetonitrile and eluent B was 0.5% acetic acid in water (1:9, v/v), with a flow rate of 1 ml/min. The standard curve for PAL glucuronidation was linear from 0.5 to 300 μM, and the correlation coefficient was >0.99. The accuracy and precision of the back-calculated values for each concentration were less than 15%.

Data Analysis. Kinetic constants for PAL glucuronidation by HLMs, HIMs, recombinant UGT1A6, or recombinant UGT1A9 were obtained by fitting experimental data to the Michaelis-Menten kinetics using Origin (OrginLab Corporation, Northampton, MA). The Michaelis-Menten equation is $v = (V_{max} \times [S])/(K_m + [S])$, where v is the rate of reaction, V_{max} is the maximum velocity, K_m is the Michaelis constant (substrate concentration at 0.5 V_{max}), and $[S]$ is the substrate concentration. The IC_{50}, representing the inhibitor concentration that inhibits 50% of control activity, was determined by nonlinear curve fitting with Origin. Kinetic constants and IC_{50} values are reported as the value ± S.E. of the parameter estimate.

Results

Analysis of PAL Metabolites. When PAL was incubated with HLMs, HIMs, and recombinant UGTs in the presence of UDPGA and the incubation mixture analyzed by HPLC, two new peaks were eluted at 5.4 (M-1) and 7.9 min (M-2), respectively (Fig. 2). These products were absent when the incubation mixture was treated with β-glucuronidase before HPLC (data not shown). The electrospray ionization mass spectra of the peaks had ions at *m/z* 313 in the negative ion mode (data not shown). These findings indicate that the peaks formed by incubating PAL in the presence of UDPGA are monoglucuronides of PAL. When PAL was incubated with human liver S9 in the presence of SAM (as a methyl donor) or PAPS (as a sulfuryl donor) and the incubation mixtures were analyzed by HPLC, no new peaks were detected in either conditions. In addition, no PAL depletion were observed in experimental groups compared with control groups (data not shown).

Kinetic Studies in HLMs, HIMs, and Recombinant UGTs. To find how many UGTs are involved, we first investigated the kinetics of PAL glucuronidation in pooled HLMs and HIMs. The substrate concentration-glucuronidation velocity curves followed typical Michaelis-Menten kinetics (Fig. 3, A and B). At the appropriate PAL concentration (average of K_m for M-1 and K_m for M-2 in HLMs, 400 μM), in a panel of commercially available rUGTs (1A1, 1A3, 1A4, 1A6, 1A7, 1A8, 1A9, 1A10, 2B7, 2B15, and 2B17), rUGT1A6 and rUGT1A9 demonstrated the ability to catalyze PAL glucuronidation (Fig. 4). Further experiments to characterize the kinetics for PAL glucuronidation revealed Michaelis-Menten kinetics for rUGT1A6 and rUGT1A9 (Fig. 5, A and B).

When PAL was incubated with HLMs, the kinetic parameters from three independent experiments over a concentration range of 25 to 2000 μM PAL were K_m = 432.7 ± 24.5 μM and V_{max} = 31.73 ± 0.74 nmol/min/mg of protein for M-1 and K_m = 336.7 ± 15.3 μM and V_{max} = 23.97 ± 0.41 nmol/min/mg of protein for M-2 (mean ± computer-calculated S.E.). Under the same condition, when HIMs were used to replace HLMs, the kinetic parameters were K_m = 626.9 ± 49.2 μM and V_{max} = 14.74 ± 0.52 nmol/min/mg of protein for M-1 and K_m = 494.3 ± 48.7 μM and V_{max} = 10.49 ± 0.43 nmol/min/mg of protein for M-2. The kinetic parameters for rUGT1A6 were K_m = 367.5 ± 25.1 μM and V_{max} = 14.12 ± 0.37 nmol/min/mg of protein for M-1 and for K_m = 211.4 ± 13.4 μM and V_{max} = 13.00 ± 0.28 nmol/min/mg of protein M-2. The kinetic

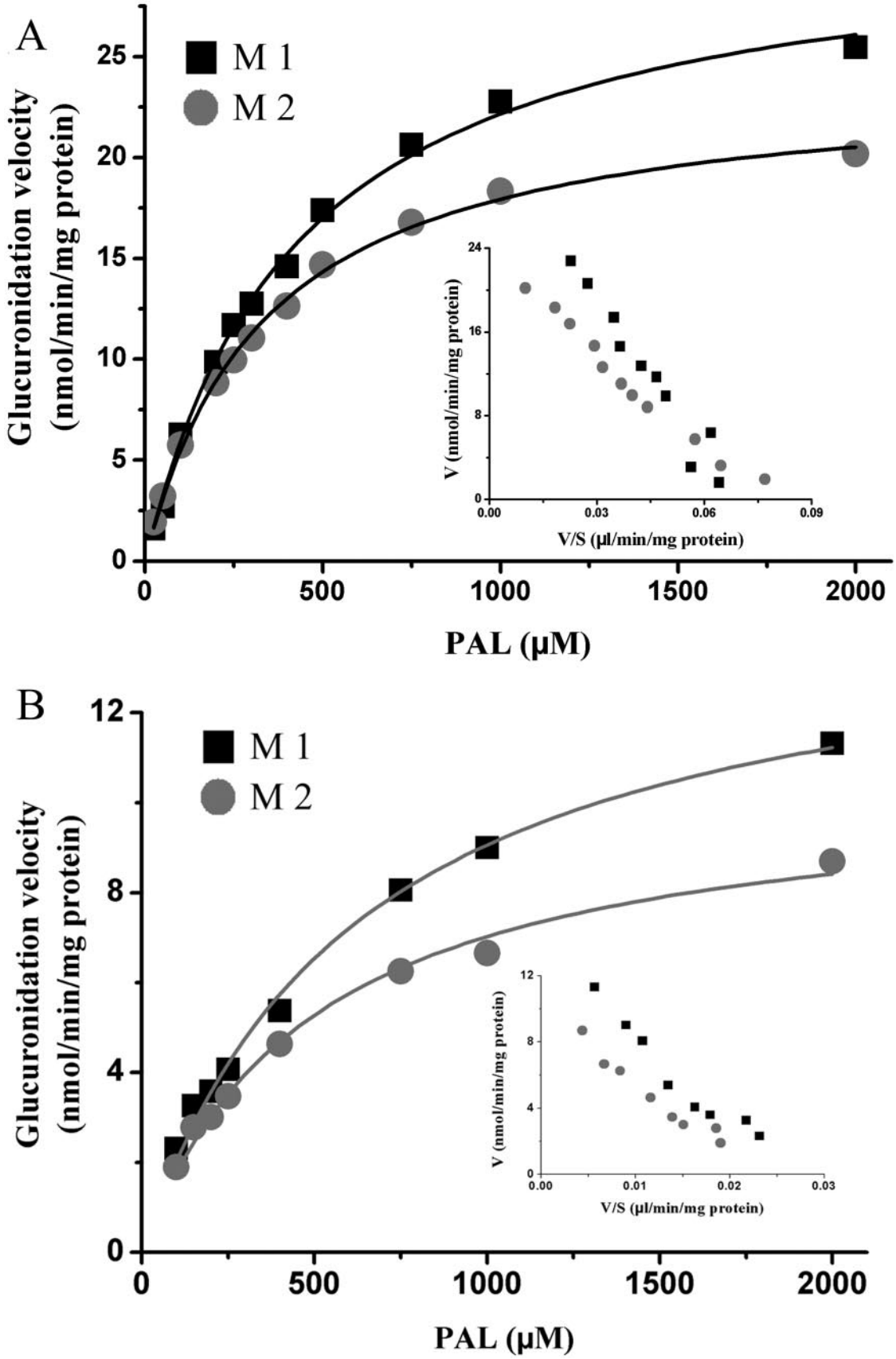

FIG. 3. Kinetics of PAL glucuronidation in HLMs (A) and in HIMs (B). PAL (25–2000 μM) was incubated with pooled HLMs (0.1 mg of protein/ml) and HIMs (0.15 mg of protein/ml) at 37°C for 20 min. The Eadie-Hofstee plot is shown as an inset. Data represent the mean of duplicate determinations.

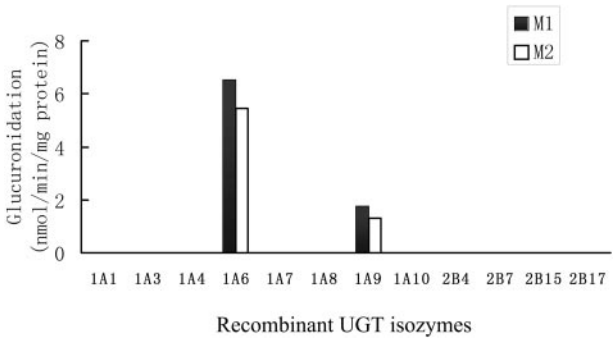

FIG. 4. PAL glucuronidation by recombinant human UGTs. PAL was incubated with recombinant human UGT1A1, UGT1A3, UGT1A4, UGT1A6, UGT1A7, UGT1A8, UGT1A9, UGT1A10, UGT2B4, UGT2B7, UGT2B15, and UGT2B17 at 37°C for 20 min. A substrate concentration of 400 μM and a protein concentration of 0.1 mg of protein/ml were used. Data represent the mean of duplicate determinations.

parameters for rUGT1A9 were K_m = 379.9 ± 42.5 μM and V_{max} = 10.03 ± 0.43 nmol/min/mg of protein for M-1 and K_m = 238.5 ± 26.2 μM and V_{max} = 9.44 ± 0.33 nmol/min/mg of protein for M-2.

Correlation Study in HLMs. The overall glucuronidation velocity of PAL (M1 + M2) in microsomes from 15 human livers ranged from 6.4 to 41.5 nmol/min/mg of protein. Rates of PAL glucuronidation correlated well (r = 0.9330, $P < 0.0001$) with rates of glucuronidation of the UGT1A6 probe substrate serotonin (Fig. 6A) but not with rates of glucuronidation of propofol (Fig. 6B), a specific probe of UGT1A9. Interestingly, the coefficient between the overall PAL glucuronidation activities and the activities toward propofol was improved to 0.7453 (from 0.2801) after addition of phenylbutazone (500 μM) to inhibit UGT1A6 activities in 15 individual HLMs (Fig. 6C).

Chemical Inhibition Studies. The inhibitory effects of phenylbutazone and androsterone on PAL glucuronidation in pooled HLMs were evaluated. As shown in Fig. 7, a similar tendency was obtained in HLMs and the rUGT1A6 system using phenylbutazone to inhibit the activity of UGT1A6. However, a different profile occurred in HLMs and the rUGT1A9 system using the 1A9 inhibitor, androsterone. The IC_{50} values for androsterone inhibition of HLMs were not determined because of the low degree of inhibition ($IC_{50} > 500$ μM), although androsterone-inhibited PAL glucuronidation by rUGT1A9 was calculated to be 27.1 ± 3.8 μM for both metabolites (mean ± computer-calculated S.E.). The IC_{50} value for phenylbutazone inhibition of HLMs was calculated to be 61.9 ± 7.9 μM for both metabolites (mean ± computer-calculated S.E.). Phenylbutazone inhibited PAL glucuronidation by rUGT1A6 to a similar extent as in HLMs, the IC_{50} value was 45.3 ± 7.7 μM for both metabolites (mean ± computer-calculated S.E.).

Discussion

The metabolism of PAL has not yet been well characterized in humans, although PAL has valuable therapeutic properties. Because the two phenol groups in PAL could be the catalytic sites of phase II conjugation enzymes such as COMTs, STs, and UGTs, in this study, we focused on investigating the conjugation pathway of PAL. Our results showed that UGTs, but not COMTs or STs, played an important role in the conjugate elimination of PAL. When PAL was incubated with HLMs, two metabolites (M-1 and M-2) were observed. These two metabolites were identified to be monoglucuronides by enzymatic hydrolysis and mass spectrometry analysis. The metabolites were not sufficient for nuclear magnetic resonance analysis; thus, their exact structure could not be ascertained.

To identify and characterize the UGT isozymes involved in PAL glucuronidation, we examined PAL glucuronidation activities in rUGT and HLM incubation systems and compared the enzyme kinetic parameters between them. In addition, both a correlation analysis and a chemical inhibition study were used to differentiate the relative contributions of the UGT isoforms involved. The kinetic profiles followed Michaelis-Menten kinetics in HIMs and HLMs incubation systems (Figs. 3 and 5). The Eadie-Hofstee plots for PAL glucuronidation by HIMs and HLMs were monophasic, suggesting that one primary UGT isozyme or more than one UGT isozymes with similar kinetic behavior would be involved in the reactions in the systems. Further experiments in 12 commercially available rUGT isozymes showed that rUGT1A6 and rUGT1A9 demonstrated catalytic activity toward PAL (Fig. 4). In addition, the K_m values of PAL of both M-1 and M-2 with rUGT1A6 were similar to those with rUGT1A9, but the values in rUGT1A6 and rUGT1A9 systems were both relatively lower than those in HLMs. It has been reported that K_m values of some substrates in rUGT isozyme systems are somewhat lower than those in HLMs (Court et al., 2003; Mano et al., 2007). Because the intrinsic clearance (CL_{int}, calculated as V_{max}/K_m) directly reflects the capability of eliminating chemicals of enzymes (De Buck and Mackie, 2007), we calculated the CL_{int} of PAL to M-1 and M-2. Both values with rUGT1A6 were higher than those with rUGT1A9, respectively. The overall activity of PAL glucuronidation was significantly correlated with the activity of serotonin glucuronidation catalyzed by UGT1A6 in 15 individual HLMs (Fig. 6A). However, the activity was not correlated with the activity toward propofol, a proposed UGT1A9-selective probe substrate (Fig. 6B). It is particularly noteworthy that after addition of phenylbutazone (500 μM), a potent inhibitor of UGT1A6, into the incubation systems, the overall PAL glucuronidation activities were significantly decreased in 15 HLMs, and the coefficient between the overall PAL glucuronidation activity and UGT1A9 activity was improved from 0.2801 to 0.7453 (Fig. 6C). In addition, the inhibitory effects of phenylbutazone on rUGT1A6- and HLM-catalyzed PAL glucuronidation had similar IC_{50} values (45.3 ± 7.7 μM versus 61.9 ± 7.9 μM). However, the UGT1A9 inhibitor androsterone (500 μM) only slightly inhibited the PAL glucuronidation activities of HLMs, although androsterone inhibited the activity of PAL glucuronidation with the IC_{50} values of 27.1 ± 3.8 μM for both metabolites in rUGT1A9 system. Furthermore, there is evidence that UGT1A6 and UGT1A9 are expressed in the liver (Strassburg et al., 1997), and UGT1A6 is a major level-expressed phenol UGT (Kessler et al., 2002). These findings suggest that although UGT1A9 has similar capability for catalyzing PAL glucuronidation to UGT1A6, the major UGT isozyme responsible for PAL glucuronidation in HLMs is UGT1A6, rather than UGT1A9, whose level in liver is probably lower than that of UGT1A6 in HLMs.

In contrast to HLMs, about one-third of the intrinsic clearance values for both metabolites were generated by HIMs. Thus, the intestine might not be the main glucuronidation metabolic organ but could contribute to presystemic elimination after oral administration of PAL. However, because no HLMs and HIMs were from the same donor, we could not measure their exact contribution. For oral administration, both the relatively higher concentration of PAL in the intestine and the larger surface area in the small intestine could contribute to elimination of PAL glucuronidation. The role of PAL glucuronidation activity in the intestine needs to be further studied.

UGT1A6 is an important UGT isozyme known to catalyze the glucuronidation of planar and short aromatic molecules, including drugs such as acetaminophen (Court et al., 2001) and valproate (Ethell et al., 2003); carcinogens, such as benzo(*a*)pyrene; and endogenous substrates, including serotonin (Krishnaswamy et al., 2003) and 5-hydroxytryptophol (Krishnaswamy et al., 2004). Up to now, human UGT1A6 has been

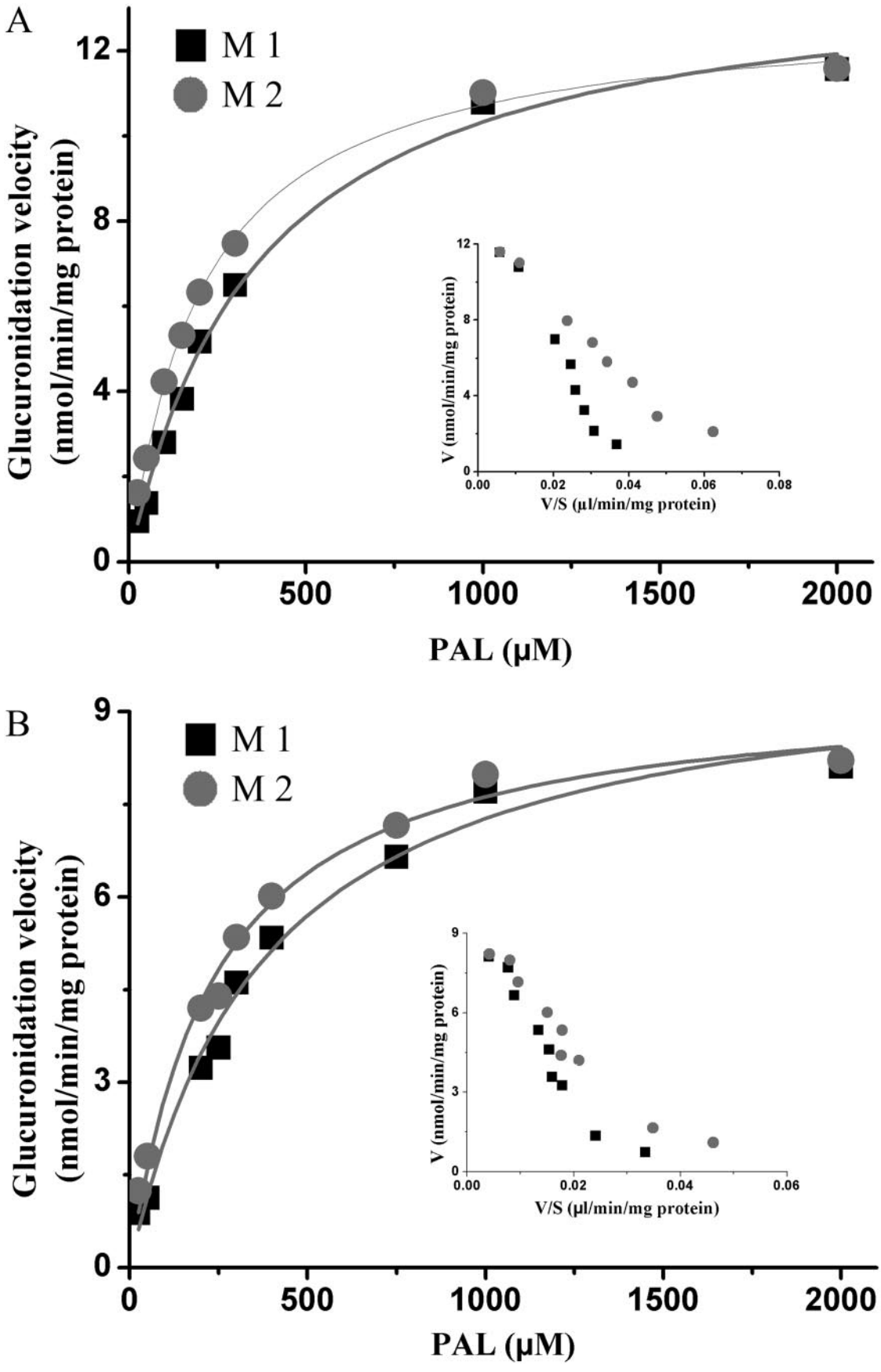

FIG. 5. Kinetics of PAL glucuronidation by recombinant UGT1A6 and recombinant UGT1A9. A, PAL (25–2000 μM) was incubated with recombinant UGT1A6 (0.1 mg of protein/ml) at 37°C for 20 min. B, PAL (25–2000 μM) was incubated with recombinant UGT1A9 (0.1 mg of protein/ml) at 37°C for 20 min. The Eadie-Hofstee plot is shown as an inset. Data represent the mean of duplicate determinations.

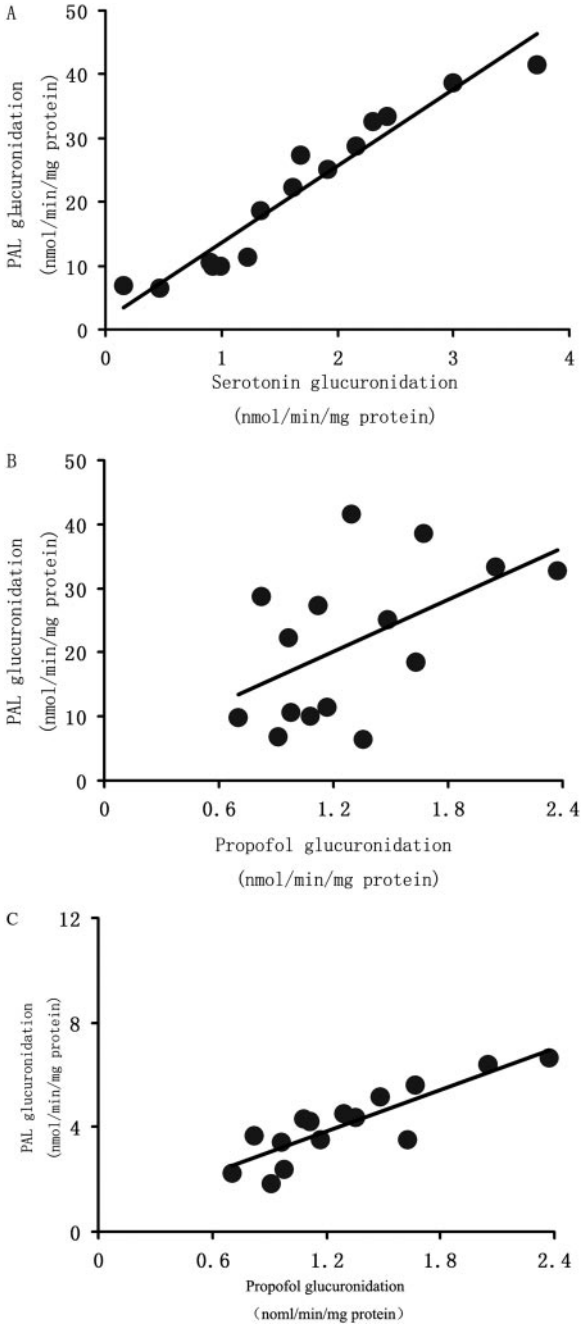

FIG. 6. Correlation between overall PAL glucuronidation and other glucuronosyltransferase activities in microsomes from 15 human livers. PAL (400 μM) was incubated with individual HLMs (0.1 mg of protein/ml) at 37°C for 20 min. Serotonin glucuronidation (A) and propofol glucuronidation (B), both typical reactions for UGT1A6 and UGT1A9, respectively, were provided by the manufacturer. C, correlation between PAL glucuronidation and propofol glucuronidation after addition of phenylbutazone (500 μM) to inhibit UGT1A6 activities in 15 individual HLMs. Data represent the mean of duplicate determinations.

identified in many tissues such as liver, kidney (Ouzzine et al., 1994), brain (Martinasevic et al., 1998; Gradinaru et al., 1999), lung (Münzel et al., 1996), and intestine (Strassburg et al., 2000). Expression of UGT1A6 has been demonstrated in human liver and in the intestine with large interindividual differences (Münzel et al., 1993). Interindividual differences in UGT1A6-mediated glucuronidation may have important toxicological, pharmacological, and physiological consequences. A number of studies have identified sequence polymorphisms within the *UGT1A6* gene that are suggested to contribute to interindividual variability. In vitro

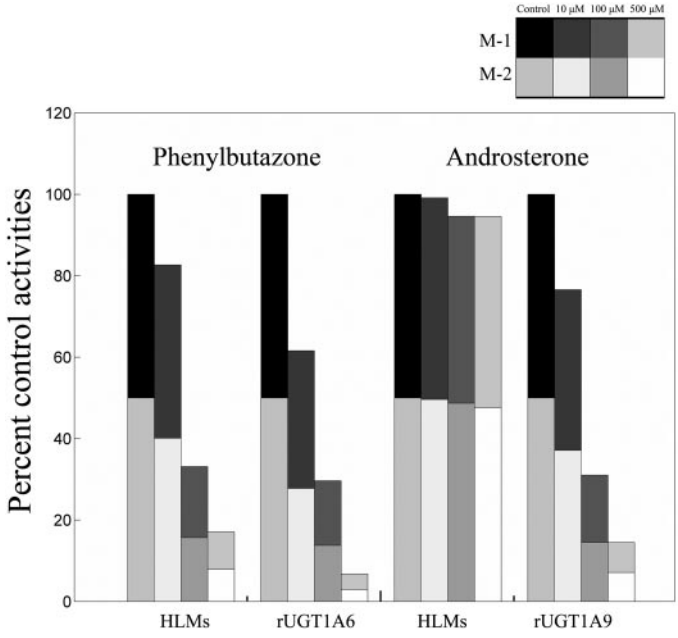

FIG. 7. Inhibitory effects of phenylbutazone on PAL glucuronidation in HLMs and recombinant UGT1A6 and androsterone on PAL glucuronidation in HLMs and recombinant UGT1A9, respectively. PAL (400 μM) was incubated with pooled HLMs (0.1 mg of protein/ml), recombinant UGT1A6 (0.1 mg of protein/ml), or recombinant UGT1A9 (0.1 mg of protein/ml) at 37°C for 20 min in the absence and presence of androsterone (0–500 μM) and phenylbutazone (0–500 μM), respectively. Data represent the mean of duplicate determinations.

expression studies of UGT1A6*2 (an isoform having two missense mutations, T181A and R184S) showed that its glucuronidation activities for phenolic compounds (4-*tert*-butylphenol, 3-ethylphenol/4-ethylphenol, 4-hydroxycoumarin, and butylated hydroxy anisole) were 27 to 75% of those for the wild-type UGT1A6*1 (Ciotti et al., 1997). More recent work (Nagar et al., 2004) indicated that the UGT1A6*2 polymorphism (allele also contains an additional amino acid substitution, S7A) was associated with approximately 2-fold higher glucuronidation activity using 4-nitrophenol and 1-napthol as substrates. Such polymorphisms would be especially important for the glucuronidation of drugs such as PAL that could be mainly UGT1A6-mediated glucuronidation.

In conclusion, we determined that UGT1A6 and UGT1A9 are involved in PAL glucuronidation and that UGT1A6 plays a major role in PAL glucuronidation in HLMs. Identification of UGT1A6 as being responsible for PAL glucuronidation will greatly improve future investigations of UGT1A6 interindividual differences associated with PAL clinical trials and the magnitude of drug-drug interactions.

References

Antonio L, Grillasca JP, Taskinen J, Elovaara E, Burchell B, Piet MH, Ethell B, Ouzzine M, Fournel-Gigleux S, and Magdalou J (2002) Characterization of catechol glucuronidation in rat liver. *Drug Metab Dispos* **30:**199–207.

Baba S, Osakabe N, Natsume M, and Terao J (2004) Orally administered rosmarinic acid is present as the conjugated and/or methylated forms in plasma, and is degraded and metabolized to conjugated forms of caffeic acid, ferulic acid and *m*-coumaric acid. *Life Sci* **75:**175–178.

Bauman JN, Goosen TC, Tugnait M, Peterkin V, Hurst SI, Menning LC, Milad M, Court MH, and Williams JA (2005) UDP-glucuronosyltransferase 2b7 is the major enzyme responsible for gemcabene glucuronidation in human liver microsomes. *Drug Metab Dispos* **33:**1349–1354.

Bosma PJ, Seppen J, Goldhoorn B, Bakker C, Oude Elferink RP, Chowdhury JR, Chowdhury NR, and Jansen PL (1994) Bilirubin UDP-glucuronosyltransferase 1 is the only relevant bilirubin glucuronidating isoform in man. *J Biol Chem* **269:**17960–17964.

Chang PN, Mao JC, Huang SH, Ning L, Wang ZJ, On T, Duan W, and Zhu YZ (2006) Analysis of cardioprotective effects using purified *Salvia miltiorrhiza* extract on isolated rat hearts. *J Pharmacol Sci* **101:**245–249.

Ciotti M, Marrone A, Potter C, and Owens IS (1997) Genetic polymorphism in the human UGT1A6 (planar phenol) UDP-glucuronosyltransferase: pharmacological implications. *Pharmacogenetics* **7:**485–495.

Court MH, Duan SX, von Moltke LL, Greenblatt DJ, Patten CJ, Miners JO, and Mackenzie PI (2001) Interindividual variability in acetaminophen glucuronidation by human liver micro-

somes: identification of relevant acetaminophen UDP-glucuronosyltransferase isoforms. *J Pharmacol Exp Ther* **299:**998–1006.
Court MH, Krishnaswamy S, Hao Q, Duan SX, Patten CJ, Von Moltke LL, and Greenblatt DJ (2003) Evaluation of 3′-azido-3′-deoxythymidine, morphine, and codeine as probe substrates for UDP-glucuronosyltransferase 2B7 (UGT2B7) in human liver microsomes: specificity and influence of the UGT2B7*2 polymorphism. *Drug Metab Dispos* **31:**1125–1133.
De Buck SS and Mackie CE (2007) Physiologically based approaches towards the prediction of pharmacokinetics: in vitro-in vivo extrapolation. *Expert Opin Drug Metab Toxicol* **3:**865–878.
Di Marco A, D'Antoni M, Attaccalite S, Carotenuto P, and Laufer R (2005) Determination of drug glucuronidation and UDP-glucuronosyltransferase selectivity using a 96-well radiometric assay. *Drug Metab Dispos* **33:**812–819.
Ding M, Ye TX, Zhao GR, Yuan YJ, and Guo ZX (2005) Aqueous extract of *Salvia miltiorrhiza* attenuates increased endothelial permeability induced by tumor necrosis factor-α. *Int Immunopharmacol* **5:**1641–1651.
Ebner T, Remmel RP, and Burchell B (1993) Human bilirubin UDP-glucuronosyltransferase catalyzes the glucuronidation of ethinylestradiol. *Mol Pharmacol* **43:**649–654.
Ethell BT, Anderson GD and Burchell B (2003) The effect of valproic acid on drug and steroid glucuronidation by expressed human UDP-glucuronosyltransferases. *Biochem Pharmacol* **65:**1441–1449.
Gradinaru D, Suleman FG, Leclerc S, Heydel JM, Grillasca JP, Magdalou J, and Minn A (1999) UDP-glucuronosyltransferase in the rat olfactory bulb: identification of the UGT1A6 isoform and age-related changes in 1-naphthol glucuronidation. *Neurochem Res* **24:**995–1000.
Guengerich PF (1989) Analysis and characterization of enzymes, in *Principles and Methods of Toxicology* (Hayes AW ed) pp 777–813, Raven Press, New York.
Han S, Liu E, and Li H (2005) On-line chemiluminescence determination protocatechuic aldehyde and protocatechuic acid in pharmaceutical preparations by capillary electrophoresis. *J Pharm Biomed Anal* **37:**733–738.
Iyanagi T (2007) Molecular mechanism of phase I and phase II drug-metabolizing enzymes: implications for detoxification. *Int Rev Cytol* **260:**35–112.
Kessler FK, Kessler MR, Auyeung DJ, and Ritter JK (2002) Glucuronidation of acetaminophen catalyzed by multiple rat phenol UDP-glucuronosyltransferases. *Drug Metab Dispos* **30:**324–330.
King CD, Rios GR, Green MD, and Tephly TR (2000) UDP-glucuronosyltransferases. *Curr Drug Metab* **1:**143–161.
Konishi Y, Hitomi Y, Yoshida M, and Yoshioka E (2005) Pharmacokinetic study of caffeic and rosmarinic acids in rats after oral administration. *J Agric Food Chem* **53:**4740–4746.
Krishnaswamy S, Duan SX, von Moltke LL, Greenblatt DJ, and Court MH (2003) Validation of serotonin (5-hydroxtryptamine) as an in vitro substrate probe for human UDP-glucuronosyltransferase (UGT) 1A6. *Drug Metab Dispos* **31:**133–139.
Krishnaswamy S, Hao Q, von Moltke LL, Greenblatt DJ, and Court MH (2004) Evaluation of 5-hydroxytryptophol and other endogenous serotonin (5-hydroxytryptamine) analogs as substrates for UDP-glucuronosyltransferase 1A6. *Drug Metab Dispos* **32:**862–869.
Lowry OH, Rosebrough NJ, Farr AL, and Randall RJ (1951) Protein measurement with the Folin phenol reagent. *J Biol Chem* **193:**265–275.
Mackenzie PI, Bock KW, Burchell B, Guillemette C, Ikushiro S, Iyanagi T, Miners JO, Owens IS, and Nebert DW (2005) Nomenclature update for the mammalian UDP glycosyltransferase (UGT) gene superfamily. *Pharmacogenet Genomics* **15:**677–685.
Mano Y, Usui T, and Kamimura H (2007) The UDP-glucuronosyltransferase 2B7 isozyme is responsible for gemfibrozil glucuronidation in the human liver. *Drug Metab Dispos* **35:**2040–2044.
Martinasevic MK, King CD, Rios GR, and Tephly TR (1998) Immunohistochemical localization of UDP-glucuronosyltransferases in rat brain during early development. *Drug Metab Dispos* **26:**1039–1041.
Münzel PA, Bookjans G, Mehner G, Lehmköster T, and Bock KW (1996) Tissue-specific 2,3,7,8-tetrachlorodibenzo-*p*-dioxin-inducible expression of human UDP-glucuronosyltransferase UGT1A6. *Arch Biochem Biophys* **335:**205–210.
Nagar S, Zalatoris JJ, and Blanchard RL (2004) Human UGT1A6 pharmacogenetics: identification of a novel SNP, characterization of allele frequencies and functional analysis of recombinant allozymes in human liver tissue and in cultured cells. *Pharmacogenetics* **14:**487–499.
Ouzzine M, Pillot T, Fournel-Gigleux S, Magdalou J, Burchell B, and Siest G (1994) Expression and role of the human liver UDP-glucuronosyltransferase UGT1*6 analyzed by specific antibodies raised against a hybrid protein produced in *Escherichia coli*. *Arch Biochem Biophys* **310:**196–204.
Radominska-Pandya A, Czernik PJ, Little JM, Battaglia E, and Mackenzie PI (1999) Structural and functional studies of UDP-glucuronosyltransferases. *Drug Metab Rev* **31:**817–899.
Strassburg CP, Kneip S, Topp J, Obermayer-Straub P, Barut A, Tukey RH, and Manns MP (2000) Polymorphic gene regulatin and interindividual variatin of UDP-glucuronosyltransferase activity in human small intestine. *J Biol Chem* **275:**36164–36171.
Strassburg CP, Nguyen N, Manns MP, and Tukey RH (1999) UDP-glucuronosyltransferase activity in human liver and colon. *Gastroenterology* **116:**149–160.
Strassburg CP, Oldhafer K, Manns MP, and Tukey RH (1997) Differential expression of the UGT1A locus in human liver, biliary and gastric tissue: identification of UGT1A7 and UGT1A10 transcripts in extrahepatic tissue. *Mol Pharmacol* **52:**212–220.
Sugiyama A, Zhu BM, Takahara A, Satoh Y, and Hashimoto K (2002) Cardiac effects of *Salvia miltiorrhiza/Dalbergia odorifera* mixture, an intravenously applicable Chinese medicine widely used for patients with ischemic heart disease in China. *Circ J* **66:**182–184.
Uchaipichat V, Mackenzie PI, Elliot DJ, and Miners JO (2006) Selectivity of substrate (trifluoperazine) and inhibitor (amitriptyline, androsterone, canrenoic acid, hecogenin, phenylbutazone, quinidine, quinine, and sulfinpyrazone) "probes" for human UDP-glucuronosyltransferases. *Drug Metab Dispos* **34:**449–456.
Xu M, Fu G, Qiao X, Wu WY, Guo H, Liu AH, Sun JH, and Guo DA (2007a) HPLC method for comparative study on tissue distribution in rat after oral administration of salvianolic acid B and phenolic acids from *Salvia miltiorrhiza*. *Biomed Chromatogr* **21:**1052–1063.
Xu M, Zhang Z, Fu G, Sun S, Sun J, Yang M, Liu A, Han J, and Guo DA (2007b) Liquid chromatography-tandem mass spectrometry analysis of protocatechuic aldehyde and its phase I and II metabolites in rat. *J Chromatogr B Analyt Technol Biomed Life Sci* **856:**100–107.
Ye G, Wang CS, Li YY, Ren H, and Guo DA (2003) Simultaneous determination and pharmacokinetic studies on (3,4-dihydroxyphenyl)-lactic acid and protocatechuic aldehyde in rat serum after oral administration of Radix *Salviae miltiorrhizae* extract. *J Chromatogr Sci* **41:**327–330.
Zhou Z, Liu Y, Miao AD, and Wang SQ (2005) Protocatechuic aldehyde suppresses TNF-α-induced ICAM-1 and VCAM-1 expression in human umbilical vein endothelial cells. *Eur J Pharmacol* **513:**1–8.

Address correspondence to: Dr. Ling Yang, Laboratory of Pharmaceutical Resource Discovery, Dalian Institute of Chemical Physics, Chinese Academy of Sciences, No. 457 Zhongshan Rd., Dalian 116023 China. E-mail: yling@dicp.ac.cn